Physico-chemical Characterization of $AlCl_3$-[EMIm]Cl Ionic Liquid Electrolytes for Aluminum Rechargeable Batteries

Chiara Ferrara[(a)], Valentina Dall'Asta[(a)], Vittorio Berbenni[(a)], Eliana Quartarone[(a)] Piercarlo Mustarelli[(a)].

(a) - Dipartimento di Chimica, Università degli Studi di Pavia, and INSTM, via Taramelli 16, 27100 Pavia, Italy.

KEYWORDS [EMIm]Cl, $AlCl_3$, aluminum batteries, aluminum electrolytes, ionic liquids, ^{27}Al NMR.

ABSTRACT

Al-ion batteries technology is getting growing attention thanks to the high natural abundance of aluminum and to the potentially high energy density that can be obtained through a 3-electrons redox process. In this work, thanks to a multi-technique approach, the ionic liquid composed by aluminum chloride and 1-ethyl-3-methyl-imidazolium chloride ([EMIm]Cl) was systematically investigated by varying the molar ratio [EMIm]Cl - $AlCl_3$ in the range 1.1 - 1.7, to obtain the best composition to be employed in a rechargeable V_2O_5-based cell. We showed that the 1.2 molar ratio composition is the best compromise between high ionic conductivity and the use of low quantity

of the highly toxic $AlCl_3$. The combined use of multinuclear (^{27}Al, ^{13}C, ^{1}H) NMR, electrochemical impedance spectroscopy (EIS), and thermal analysis allowed us to shed light on the structure-properties relationships of this complex system, also resolving some controversial conclusions of previous literature.

Keywords: aluminum batteries, $AlCl_3$, ([EMIm]Cl, NMR, EIS

INTRODUCTION

The major challenge in the field of Aluminum Ion Batteries, AIBs, is the research for Al^{3+} conducting electrolytes with good transport properties at room temperature. Ionic liquids, ILs, based on organic components and aluminum salts represent the state of the art in this field since the moment of their first introduction [1-4]. During the past decades, several different systems were proposed as electrolytes for Al secondary batteries, ranging from aprotic polar organic solvents previously used for Li and Na batteries [5-6], to molten salts eutectics [7], and dual electrolytes based on combination of the just mentioned systems. The use of organic solvents is limited by the very low solubility of Al(III) salts, as well as by issues related to volatility and low thermal stability. The introduction of additives does not eliminate completely this problem [5-6]. On the contrary, ionic liquids (ILs) present high thermal stability, ability to dissolve a wide range of compounds thanks to their strong electrostatic interactions, low volatility and flammability, low toxicity, and ability to remain liquid at the room temperature (room temperature ionic liquids, RTILs) [8].

Different ILs compositions were proposed in the recent years [3,9,10]. The selection of $AlCl_3$ as aluminum (III) source was based on its better stability with respect to Br- and I-containing species [11]. Regarding the organic component, several different molecules were investigated including (1-butyl-1-methyl pyrrolidinium bis(trifluoromethylsulfonyl)imide, 1-ethyl-3-methylimidazolium bis(trifluoromethylsulfonyl)amide, trihexyl-tetradecyl-phosphonium bis(trifluoromethylsulfonyl)amide, dicyanamide and 4-propylpyridine [12-15], but the main and most employed system is indeed the IL based on 1-ethyl-3-methylimidazolium chloride ([EMIm]Cl), which provides very low vapor pressure, high electrical conductivity, wide stable electrochemical window, and liquid state in a large composition range [9,16]. These

chloroaluminate electrolytes are classified as acidic, neutral and basic depending on the $AlCl_3$ content. In particular, if the $AlCl_3$ content is less than 50 mol% the electrolytes contain $AlCl_4^-$ and Cl^- moieties and possess basic characteristics, whereas for content greater than 50 mol% the electrolytes are based on the presence of $AlCl_4^-$ and $Al_2Cl_7^-$ species, and have acidic properties. Only the acidic compositions are active for Al plating and stripping at the anode, according to the reversible reaction $4Al_2Cl_7^- + 3e^- \leftrightarrow Al + 7AlCl_4^-$ [16,17]; in contrast, the basic compositions do not show good electrochemical activity. Different studies demonstrated the good electrochemical performances of these electrolytes in combination with different electrodes [6,16,18]. At the same time, these ILs present also significant limitations related to their highly corrosive nature, high viscosity and hygroscopicity, and significant toxicity chiefly due to the aluminum salt. At some extent, these issues can be managed by tuning the composition, in order to obtain a good compromise between transport properties and the abovementioned detrimental aspects. Finally, although the chloroaluminate ILs are widely employed in the research for new AIBs, to date scarce attention has been devoted to the investigation of their structure/properties relationships, and many controversial aspects still need to be addressed, including careful speciation of ionic moieties present at the different compositions.

In this work, we report a systematic investigation on the $AlCl_3$/([EMIm]Cl system. The molar composition $AlCl_3$:[EMIm]Cl was explored in the acidic range 1.1-1.7. Our multi-techniques approach, including multinuclear NMR, electrochemical impedance spectroscopy (EIS) and thermal analysis allowed us to obtain a careful description on the system, including speciation of ionic moieties. We were able to identify the best compositional range, and tested one of the optimal mixtures in an electrochemical cell with aluminum as the anode and standard V_2O_5 as the cathode.

EXPERIMENTAL

Synthesis of $AlCl_3$/[EMIm]Cl Ionic Liquids (ILs) - The ionic liquids were prepared by mixing $AlCl_3$ (anhydrous, powder, 99.99%, Sigma Aldrich) and 1-ethyl-3-methyl-imidazolium chloride ([EMIm]Cl) (98%, Sigma Aldrich), in various $AlCl_3$/[EMIm]Cl molar ratios, namely: 1.1, 1.2, 1.3, 1.4, 1.5 and 1.7. In detail, $AlCl_3$ was added to [EMIm]Cl very slowly to prevent heating due to the strongly exothermic reaction (temperature always under 50°C) and under vigorous magnetic stirring, inside an argon-filled glove-box (MBraun, O_2 and H_2O levels < 1 ppm). 4Å-molecular sieves were added to the ILs to keep them dry. In the following the samples will be named as "1.n ILs" (e.g. "1.1 IL" means the $AlCl_3$/[EMIm]Cl 1.1 molar composition).

Thermal Analysis - Differential Scanning Calorimetry (DSC) measurements were carried out on all the ILs and on the pure [EMIm]Cl, using DSC Q2000 (TA Instruments). For each composition, ~6-7 mg were weighed inside the glove-box and sealed into Al pans, to perform the thermal treatment. For the ILs the treatment was made of 3 steps: 1) cooling from room temperature to -70°C with a cooling ramp of 5°C/min, 2) waiting at -70°C for 1 min, 3) heating up to +90°C with a heating ramp of 10°C/min. For the pure [EMIm]Cl, which is solid at r.t., the treatment consisted in heating the compound up to 180°C using a heating ramp of 10°C/min. The enthalpies associated to melting and crystallization processes were obtained by integration of the area of the DSC peaks, with the TA Universal Analysis Software.

Conductivity measurements - The ionic conductivity data for all the ILs were obtained by performing Electrochemical Impedance Spectroscopy (EIS) measurements by means of a Frequency Response Analyzer (FRA - Solartron 1255) connected to an Electrochemical Interface (Solartron 1287) over the frequency range 0.1 Hz - 10^5 Hz, with a voltage of 100 mV. EIS measurements were performed in the range from -10°C to +90°C. The samples were let to equilibrate at each selected temperature in an oil bath for at least 1 hour before starting the EIS

measurement. An exception was done for the IL with 1.1 molar ratio, that was tested from 0°C to 90°C, because of its crystallization temperature near -10°C. The EIS data were recorded using a home-made cell, composed by a sealed brown glass vial with two inner planar platinum electrodes. Before carrying out the measurements directly on the ILs, the cell was calibrated by performing an EIS measurement at 25°C with KCl 0.1 M solution, ($\sigma_{\text{KCl 0.1M (25°C)}}$ = 0.01288 S cm^{-1}).

The Vogel-Tamman-Fulcher (VTF) equation was applied to fit the experimental data sets of ionic conductivity in the temperature range from -10°C to +90°C, for all the different electrolyte compositions ranging from 1.2 to 1.7:

$$\sigma(T) = \sigma_0 \cdot e^{-\frac{B}{T-T_0}} \qquad \text{Equation 1}$$

$\sigma(T)$ is the ionic conductivity, σ_0 is the pre-exponential factor, B is a pseudo-activation energy, T is the current temperature, and T_0 is a parameter which can be interpreted as the ideal glass transition temperature, and lies 20-50 K below the glass-transition temperature, T_g, as determined by standard DSC measurements. From the fitting of the data, the values of B and of T_0 were extracted.

For the 1.1 composition, the experimental data were fitted with the Arrhenius equation

$$\sigma(T) = \sigma_0 \cdot e^{-\frac{E_{att}}{RT}} \qquad \text{Equation 2}$$

where E_{att} is the activation energy for ions motion, and R is the gas constant.

NMR measurements - The NMR spectra were acquired at 104.23 MHz on a 9.4 T (400.13 MHz) Bruker Avance III spectrometer at ambient temperature. ^{1}H quantitative one-pulse spectra were collected with a pulse length of 14 μs, recycle delay of 4 s and 32 scans. ^{13}C HPDEC spectra were

collected under high power decoupling to ensure high resolution with pulse length on ^{13}C of 11 μs, recycle delay of 20 s and 2k scans. ^{27}Al quantitative one-pulse spectra were acquired with a π/2 pulse of 9 μs, 5 second of recycle delay and 1k scans. Pulse lengths and recycle delay were carefully calibrated to ensure the full relaxation of the magnetization. The pre-acquisition delay was fixed to … in order to minimize… Chemical shifts for ^{1}H and ^{13}C were referred to TMS (0 ppm in both case) using adamantane as the secondary standard, whereas the signal of 1 M aqueous solution of $Al(NO_3)_3.9H_2O$ (0 ppm) was used as the reference for ^{27}Al. Spectral analysis was performed with DMFit program [19]. All the manipulations of the samples were carried out under inert atmosphere, and the measurements were performed immediately after samples preparation, in order to minimize reactions with moisture, or after given times as reported in the Results and Discussion section.

Electrochemical tests - Cyclic voltammetry (CV) was performed by means of an Autolab PGSTAT 30 (Eco Chemie), by applying a potential scan rate of 0.1 mV/s in the potential range 0.01 V - 0.9 V, on a cell with the following configuration: Al (RE, CE) / 1.2 IL / V_2O_5 (WE). Here RE, CE and WE indicate Reference, Counter and Working Electrodes, respectively. Three glass microfiber filters GF/C were used as separators. Galvanostatic cycling was carried out in the same potential range and on the same cell configuration employed in the CV. Three different current densities were imposed, and namely: 22, 44 and 222 mA g^{-1}. The capacity of vanadium oxide was calculated by the mass of the active material contained in the cell. The WE was prepared by mixing 80 wt% of vanadium oxide powder, 10 wt% of carbon black (Vulcan XC 72R Cabot Corp.) and 10 wt% poly(tetrafluoroethylene) 35 μm particle size (Sigma Aldrich) in N-methyl-2-pyrrolidinone (99%, Sigma Aldrich). The resultant slurry, after 6 hours under magnetic stirring at room temperature, was tape-casted onto a nickel foil 0.01 mm thick (99.95%, Alfa Aesar) by means of a home-made

doctor blade. After drying it at room temperature overnight, and then at 120°C in vacuum for 6 hours, the cathode was transferred into the Ar-filled glove-box, and cut into disks with an area of 0.785 cm^2.

RESULTS AND DISCUSSION

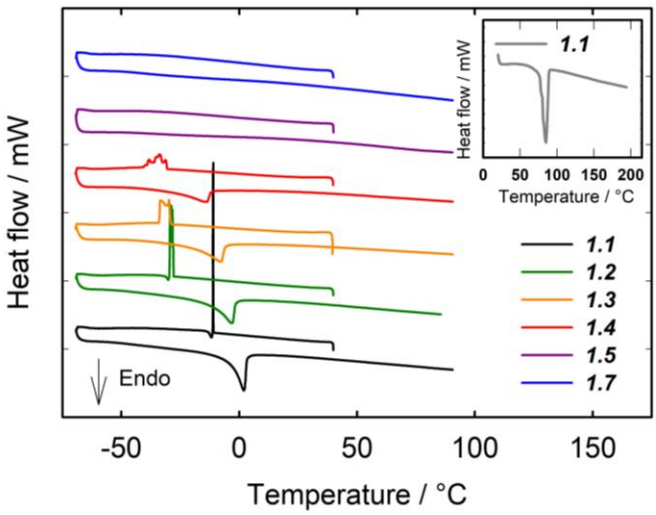

Figure 1. DSC thermograms of the ILs. In the inset, the thermal trace of the pure [EMIm]Cl is reported. (DEVI TOGLIERE LA SCRITTA 1.1 NELL INSET)

	Composition

	[EMIm]Cl	1.1	1.2	1.3	1.4	1.5	1.7
mol% $AlCl_3$	0	52.38	54.55	56.52	58.34	60.00	62.96
T_c (K)	--	262.17	244.98	243.40	242.55	--	--
ΔH_c (J/g)	--	39.73	32.27	22.93	17.39	--	--
T_m (K)	354.01	269.57	260.93	252.98	244.14	--	--
ΔH_m (J/g)	78.92	38.00	29.00	23.85	16.90	--	--

Table 1. Physico-chemical properties of [EMIm]Cl powder and $AlCl_3$/[EMIm]Cl compositions with various molar ratios. T_c =crystallization temperature; T_m = melting temperature; ΔH_c crystallization enthalpy; ΔH_m = melting enthalpy.

Figure 1 shows the DSC results for pure [EMIm]Cl and all the prepared ILs. The corresponding physico-chemical data are reported in Table 1. Pure [EMIm]Cl displays a neat melting peak near 80°C, with a specific melting enthalpy of about 79 J/g. The addition of $AlCl_3$ gives origin to RTILs for all the examined compositions. In particular, the 1.1 composition shows very sharp crystallization and melting features at -10°C and -3°C, respectively. The value of melting enthalpy is strongly reduced with respect to pure [EMIm]Cl, which demonstrates the decrease of the lattice energy leading to the formation of RTILs. Glass transitions are not observed in the explored temperature range. Further addition of $AlCl_3$ up top 1.4 molar ratio leads to the monotonous decrease of both ΔH_c and ΔH_m, accompanied by a progressive enlargement of both the endo- and exothermic features. This means that the samples become less ordered, likely because of the increase of the bulky $Al_2Cl_7^-$ moieties [15, 16] (see below NMR results). However, no glass

transition phenomena, T_g, are observed for all these samples. 1.5 and 1.7 compositions are in the liquid state in the entire temperature range, as expected for systems with high level of disorder [20-23]. Also in this case, however, no clear T_g features could be found, either because falling below the available temperature range, or because the liquids are too "strong" (in the sense of Angell's fragility concept) [24] to allow T_g observation in the timescale of the DSC experiment (~1 min).

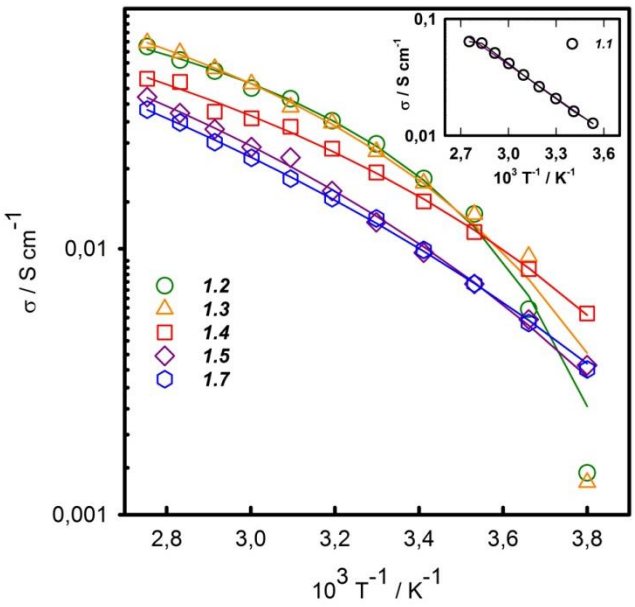

Figure 2. Arrhenius plots of the ionic conductivity of all the investigated compositions, together with their best-fits (Arrhenius for 1.1 IL, and VTF for 1.2-1.7 ILs). Errors are inside the symbols dimensions. (CI SONO ANCORA LE VIRGOLE!)

	Composition				
	1.2	**1.3**	**1.4**	**1.5**	**1.7**
R^2 VTF fit	0.9973	0.9960	0.9895	0.9971	0.9991
B (K)	135.61	230.74	301.87	460.36	558.18
T_0 (K)	230.15	207.85	182.10	166.37	146.16

Table 2. Parameters of the VTF fit. R^2: Pearson coefficient of the best-fit; B: pseudo-activation energy; T_0: ideal glass transition temperature.

Figure 2 displays the behaviour of the ionic conductivity vs. temperature for the investigated samples. 1.1 composition shows a clear Arrhenius behaviour (see inset) with activation energy, E_a = 0.19 eV. Arrhenian behaviours are typical of crystalline conductors or amorphous phases below the T_g. In our case, we can rationalize this unusual behaviour with the relatively ordered nature of 1.1 IL also in the liquid state, which is revealed by DSC results of Figure 1. ILs with compositions from 1.2 to 1.7 display a clear VTF behaviour, as generally expected for samples in the liquid state, where disorder and/or free volume become predominant [22]. The VTF best-fits parameters are reported in Table 2. The increase of $AlCl_3$ content determines the increase of the pseudo-activation energy and a decrease of T_0, in agreement with the results reported by Vila et al. [25].

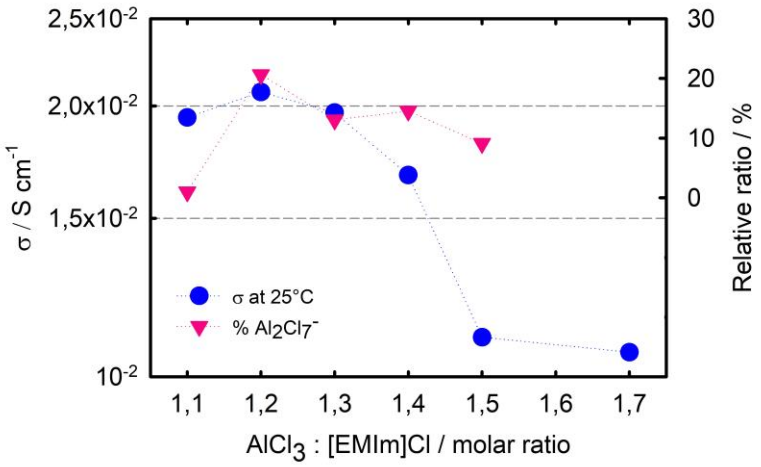

Figure 3. Ionic conductivity at 25°C of all the tested ILs (blue circles), and fraction of $Al_2Cl_7^-$ moiety (pink triangles) as obtained by best-fits of ^{27}Al NMR spectra (see following). (CI SONO ANCORA LE VIRGOLE! METTI "$Al_2Cl_7^-$ FRACTION" INVECE DI "RELATIVE RATIO")

Figure 3 shows the conductivity values at 25°C of all the tested ILs, together with the fraction of $Al_2Cl_7^-$ moiety as determined by ^{27}Al NMR (see following). Values in the range 10-20 mS cm^{-1} are typical of [EMIm]Cl-$AlCl_3$ electrolytes (see ref 26 and references therein). We observed a plateau in the compositional range 1.1-1.3 followed by a decrease for higher $AlCl_3$ contents. This behavior of the conductivity can be clearly related to the ratio between $AlCl_4^-$ and $Al_2Cl_7^-$ moieties as determined by means of ^{27}Al NMR measurements reported in Figure 3. This point will be addressed in the following.

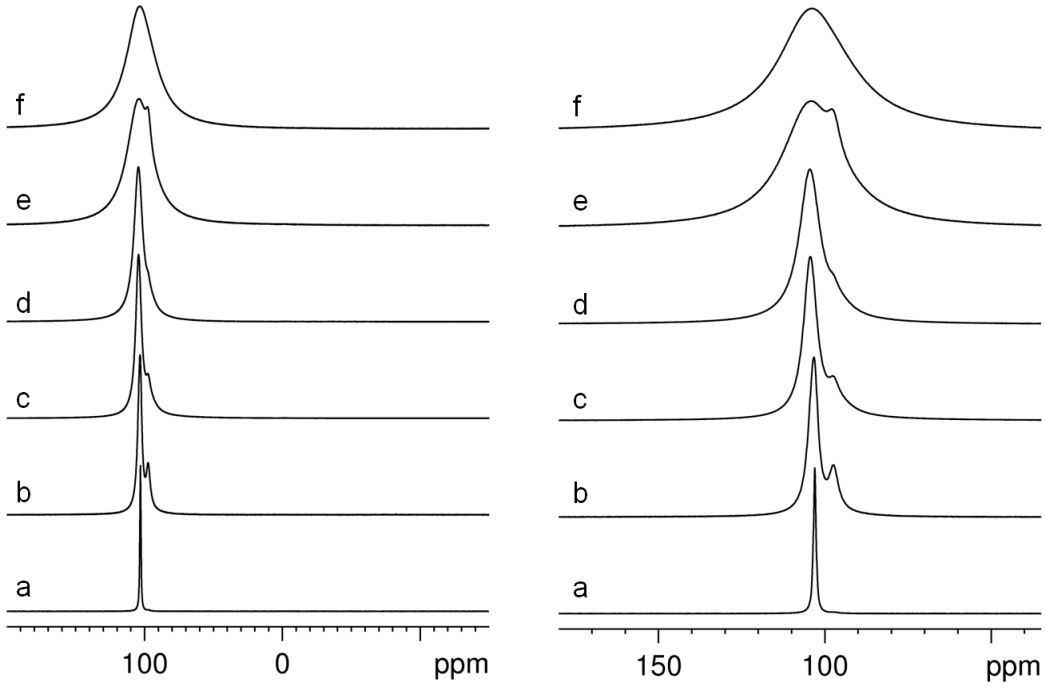

Figure 4. ^{27}Al NMR spectra for the 1.1 (a), 1.2 (b), 1.3 (c), 1.4 (d), 1.5 (e) and 1.7 (f) compositions in the 200 / -150 ppm range (left) and their zoom in the 180 / 40 ppm range (right).

Figure 4 reports the ^{27}Al NMR spectra for all the samples in the composition range 1.1-1.7. In all cases it is possible to observe two signals at ~103 ppm and ~97 ppm; no other features appear in all the explored chemical shift range (500 / -500 ppm). The NMR spectra do not show relevant chemical shifts as a function of the composition, whereas significant line-width changes are observed moving from 1.1 to 1.7 compositions, and this variation is more marked for the peak observed at 103 ppm. ^{13}C and ^{1}H spectra were also acquired (see Figure S1), which presented only signals fully compatible with liquid [EMIm]Cl, so confirming that chemical reactions did not occur between the organic molecule and the Al salt.

Therefore, the two peaks observed in the ^{27}Al spectra must be attributed to inorganic Al species. Moreover, we can exclude the presence of unreacted solid, as signal of solid $AlCl_3$ was reported at -1.6 ppm [15]. Several ^{27}Al NMR studies on the Al complexes in solution or in ionic liquids were reported in the past (MEGLIO ANTICIPARE QUI TUTTI I RIFERIMENTI NECESSARI). Similar spectra were already reported for the $AlCl_3$/[EMIm]Cl system, although not for the complete series of samples vs. composition. [11, 15,16]. Following these works, the peaks at 103 ppm and 97 ppm can be tentatively assigned to $AlCl_4^-$ and $Al_2Cl_7^-$, respectively. However, the literature data are controversial, and the attribution of these resonances is not straightforward. For the correct attribution of the observed signals, all the present species and equilibria, due to the presence of $AlCl_3$ and Cl^-, relative to the acidic compositions must be considered:

$AlCl_3 + Cl^- \rightarrow AlCl_4^-$ Equation 3

$AlCl_4^- + AlCl_3 \rightarrow Al_2Cl_7^-$ Equation 4

All the previous studies attributed the signal observed at 103 ppm to $AlCl_4^-$ species [27-30], and no significant variations in the chemical shift of this species were reported when changing compositions, concentrations or solvents. The chemical shift attribution of the signal due to $Al_2Cl_7^-$ clusters is more controversial. Previous studies suggested that fast kinetic of the $AlCl_4^-/Al_2Cl_7^-$ equilibrium with respect to the NMR measurement timescale would lead to the impossibility to distinguish the two signals [27,28]. Attempts to discriminate the two species were performed by varying the pre-acquisition delay time [27], and the unique observed signal was attributed to both the $AlCl_4^-/Al_2Cl_7^-$ anions under rapid exchange. A subsequent work by Takahashi et al. confirmed this result, indicating that the resonance obtained at 97 ppm could be attributed to undesired reaction products between Al moieties and moisture [28]. In that work a single main resonance

was observed at 103 ppm, whereas a minor feature (around 0.3%) was found at 97 ppm. Moreover, this last peak was observed only for two samples out of the five examined, and there was not any evident trend between the its intensity and the nominal composition.

On the contrary, our measurements revealed the presence of two clearly detectable sites for all the compositions, and the percentage of the peak at 97 ppm was always higher than 0.5%, reaching 20% for the 1.2 sample. Similar results were reported by Wilkes et al. [29] for the same system $AlCl_3$/[EMIm]Cl in the acidic melt compositional range.

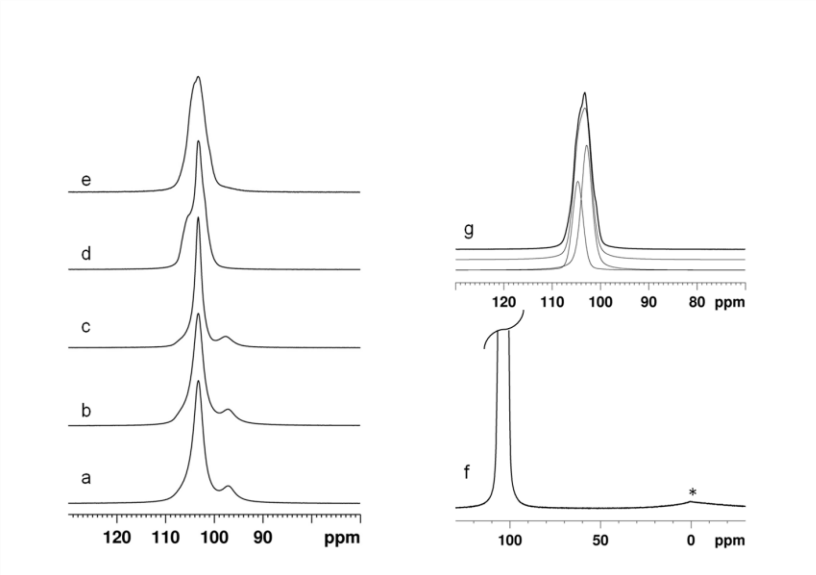

Figure 5. ^{27}Al spectra acquired for 1.2 composition as prepared and sealed under Ar (a), and after exposure to air for 30 s (b), 150 s (c), 200 s under gentle mixing (d), and 300 s under gentle mixing with addition of a small amount of H_2O (e). The f panel shows the spectrum (e) in the chemical shift range 130 / -20 ppm highlighting the feature at ~0 ppm (*). The best-fit of the spectrum (e) is presented in panel g together with the two components at 105 and 103 ppm.

In order to attribute univocally the NMR peaks to the anion species, we evaluated the formation of byproducts due to presence of water in the system. To this aim, the 1.2 composition (showing the biggest resonance at 97 ppm) was exposed to ambient air (relative humidity ~60%), with possible addition of liquid water, for different time intervals. The results are reported in Figure 5. The intensity of the peak at 97 ppm decreased by increasing the exposure time to air; at the same time, a shoulder emerged at 105 ppm (see Figure 5 d-e). With the further addition of water (~1 mm^3, with respect to ~300 mm^3 of sample), we observed a further increase of the intensity of the peak at 105 ppm, which merged with that at 103 ppm, as revealed by spectral deconvolution (Figure 5g). Moreover, a small resonance appeared at ~0 ppm (Figure 5f). In the frame of the previous peaks assignment, all this spectral evolution can be rationalized in terms of consumption of the $Al_2Cl_7^-$ anion due to $AlCl_4^-$ subtraction from the Equilibrium 4 by hydrolysis. In fact, the peak at 97 ppm decreases with time exposure to moisture. At the same time, the appearance of the peak at 105 ppm can be assigned to hydrolysis products $[AlCl_{4-n}(OH)_n]^-$ relative to the reaction between $AlCl_4^-$ and H_2O. The addition of liquid water determines also formation of $Al(OH)_{3-x}O_{3-x/3}$ solid products, clearly visible in the sample as white crystals, which give origin to the small peak at ~0 ppm observed in Figure 5f.

Previous detailed NMR investigations on the hydrolysis product of $AlCl_3$ were presented by Černý et al. [30-31]. These studies identified the resonance observed at 100 ppm as the signal of the $AlCl_4^-$ species and attributed the peak at 97 ppm to the $AlCl_3(OH)^-$ anion due to the presence of undesired traces of H_2O. A detailed analysis of hydrolysis products allowed to assign the different NMR peaks to the $Al(OH)_{4-n}Cl_4^-$ species. Signals ranging from 97 ppm for $AlCl_3(OH)^-$ to 79 ppm for $Al(OH)_4^-$, were attributed based on the different electronegativity of the two ligands (OH^- and Cl^-). However, it must be considered that the solvents selected for these studies were benzene and

n-heptane, i.e. apolar organic solvents presenting lower solvating power with respect to the $AlCl_3$ salt. In the present work the system under study is significantly different, as the $AlCl_3$/[EMIm]Cl is a polar ionic liquid with largely different dielectric properties.

Based on our results, the two resonances can be unambiguously attributed to $AlCl_4^-$ (103 ppm) and $Al_2Cl_7^-$ (97 ppm) anions. This conclusion is supported by further evidences. The presence of a ^{27}Al resonance at 97-91 ppm was related to the Al_2Cl_6 dimers D_{2h} symmetry with two $AlCl_4$ units connected via Cl-Cl edge in molten $ReCl_3$-$AlCl_3$ [32] and Al_2Cl_6 in toluene [33]. Recent works on ionic liquids based on $AlCl_3$/[EMIm]Cl and $AlCl_3$/RR'SO_2 compositions further support this interpretation, presenting attributions and ratios between the two peaks which are similar to those reported in the present study [10,11,34].

Best-fit analysis of the NMR spectra allowed to evaluate the relative amounts of the two species. The results are reported in Figure 3 and in Table 3, together with the other best-fit parameters. The concentration of $Al_2Cl_7^-$ reaches a maximum for the 1.2 composition, and decreases for higher concentrations. Due to the featureless nature of 1.7 spectrum, in this case the best fit procedure was not performed. From Figure 3 it is evident that the maximum of ionic conductivity corresponds to the maximum of $Al_2Cl_7^-$ moiety in the IL. This is in agreement with previous literature (REF). In fact, even if both the species were reported to be electrochemically active, the $Al_2Cl_7^-$ anion seemed to be the major ionic transport carrier [10].

Sample	**δ_{iso} / ppm**		**Broadening / Hz**		**xG/(1-x)L**		**%**	
	$AlCl_4^-$	$Al_2Cl_7^-$	$AlCl_4^-$	$Al_2Cl_7^-$	$AlCl_4^-$	$Al_2Cl_7^-$	$AlCl_4^-$	$Al_2Cl_7^-$
1.1	103.2	97.2	88.4	155.2	0	0	99.0	1.0
1.2	103.5	97.3	359.9	367.7	0	0	79.4	20.6

1.3	104.4	97.1	502.1	550.2	0	0	86.9	13.1
1.4	104.7	96.9	789.3	576.7	0	0	85.5	14.5
1.5	104.8	97.0	2075.2	632.3	0	0	90.9	9.1

Table 3. NMR parameters obtained by best-fitting the spectra with two components attributed to $AlCl_4^-$ and $Al_2Cl_7^-$ species; all the fitting parameters were allowed to freely move during the fitting procedure. Errors in the percentage evaluation are below 2%.

Additional information can be obtained from the analysis of the NMR line-width. The line-width, $\Delta\nu$, of the two peaks at 103 and 96 ppm monotonously increases with the increase of $AlCl_3$. This behavior was early observed by Gray and Maciel [27], and attributed to the increase of quadrupolar spin-spin relaxation rate, $(1/T_2)_Q$, which, in the extreme narrowing regime (ENR), is given by the relationship

$$\left(\frac{1}{T_2}\right)_Q = \frac{3}{10}\pi^2 \frac{2I+1}{I^2(2I-1)} C_Q^2 \left(1+\frac{\eta^2}{3}\right)\tau_c \qquad \text{Equation 5}$$

where $1/T_2 \cong \pi\Delta\nu$, C_Q is the quadrupolar coupling constant, η is the quadrupolar asymmetry parameter, τ_c is the correlation time, and I is the spin number (I = 5/2 for ^{27}Al). Here, the ENR condition is demonstrated by the absence of quadrupolar features and by the full Lorentzian shape of both the NMR peaks, which is typical of liquids (see Table 3). Under ENR conditions, the quadrupolar coupling constant of the two Al-based species only depends on their molecular structure [36]. Therefore, the line-width increase with composition only depends on the correlation time, which in turn is related to the ion mobility. In particular, $AlCl_4^-$ species shows the most significant broadening, which passes from ~88 Hz to ~2000 Hz. In contrast, the $Al_2Cl_7^-$ line-width

is subjected to only a minor variation passing from 1.1 to 1.5 sample (~155 and ~630 Hz, respectively). From these ^{27}Al NMR data, we can conclude that the $Al_2Cl_7^-$ moiety is more mobile than $AlCl_4^-$. The conductivity maximum of Figure 3 is therefore given by the interplay between the $Al_2Cl_7^-$/ $AlCl_4^-$ ratio and the relative mobility of the species.

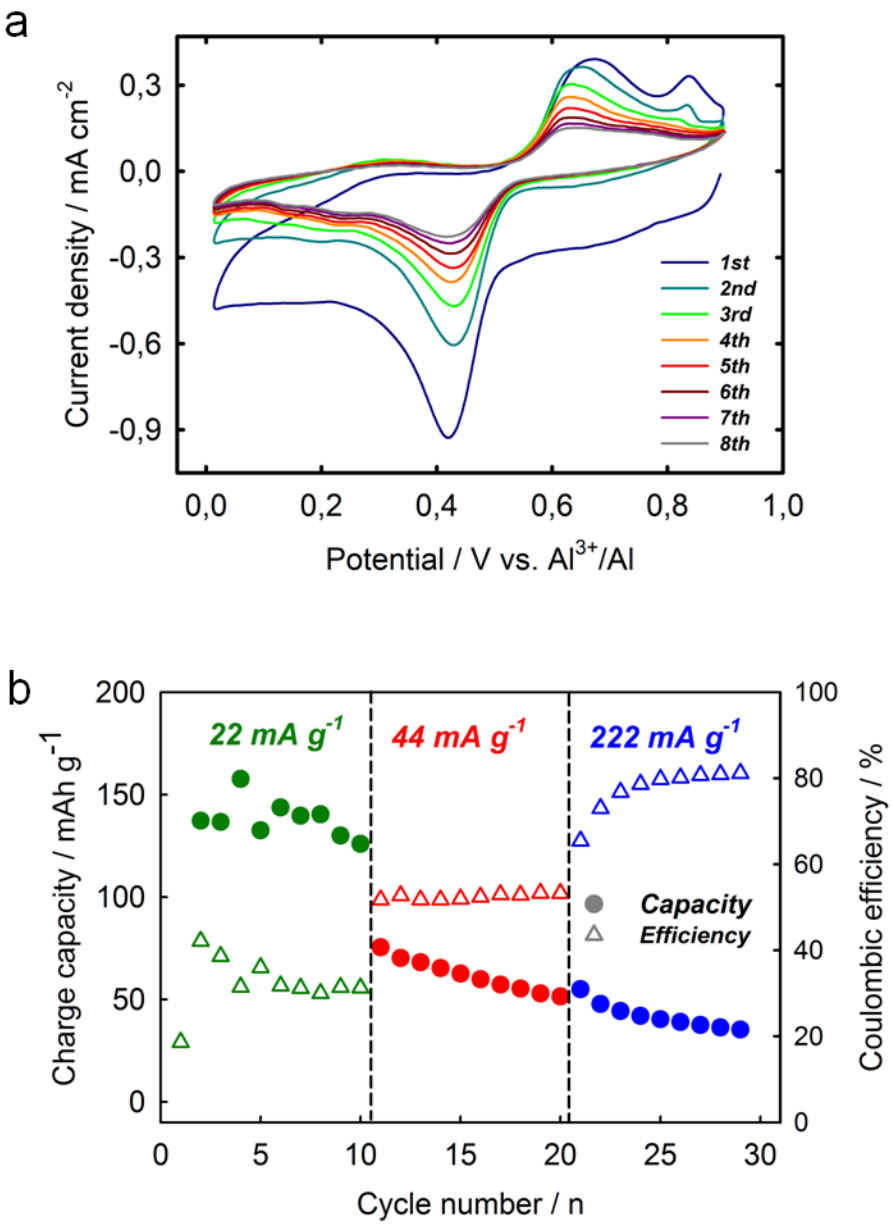

Figure 6. Electrochemical performances of the 1.2 IL in an Al-ion cell: a) Cyclic voltammetry of V_2O_5 cathode (8 cycles) at a scan rate of 0.1 mV s^{-1} between 0.01 V and 0.9 V; b) Charge capacity (full symbols) and % coulombic efficiency (empty symbols) vs. cycle number of the V_2O_5 composite cathode at various applied current densities (22, 44 and 222 mA g^{-1}).

Based on thermal, conductivity and NMR analyses, the composition 1.2 was chosen for electrochemical tests and used as the electrolyte for AIBs in half-cell configuration, employing a vanadium oxide cathode, prepared from commercial V_2O_5 powder. The feasibility of the system was verified through cyclic voltammetry (CV) and galvanostatic cycling at different current densities, as reported in Figure 6.

From the CV curves (Figure 6a) it can be clearly seen the reversibility of the aluminium insertion/de-insertion into the cathode active material (the peak at 0.85 V, taking place only in the first and second cycles, may be related to impurities or to a SEI formation). The current density stabilization is fully reached at the 7th cycle, as the curves in the 7th and 8th cycles are overlapped. The galvanostatic cycling is carried out at three increasing current gravimetric densities, namely 22, 44 and 222 mA g^{-1}, as reported in Figure 6b. At low current, the charge capacity is outstandingly high: it approaches the value of 127 mA h g^{-1} at the 10th cycle performed at 22 mA g^{-1}. Interestingly, despite of the expected capacity fading when increasing the current value, the system is still able to develop ~50 mA h g^{-1} when the applied current density is very high (222 mA g^{-1}). As already reported in literature for similar systems [41], the coulombic efficiency is poor. Anyway, it increases while increasing the current value, and overcomes the value of 80% at the end of the high current cycling.

CONCLUSIONS

In this paper, we reported a thorough physico-chemical investigation of the system $AlCl_3$ - [EMIm]Cl, which is of interest as possible electrolyte in Al-ion rechargeable batteries. In detail, we explored the acidic region for molar contents in the range 1.1-1.7. By means of careful ^{27}Al NMR experiments, we assigned univocally the two resonances at 103 and 97 ppm to $AlCl_4^-$ and $Al_2Cl_7^-$ moieties, respectively, whereas in the past there has been a strong debate about the nature of the peak at 97 ppm, if observed. By best-fitting the NMR features, we found a clear trend between the transport properties of the ILs and the ratio $Al_2Cl_7^-/AlCl_4^-$. Moreover, by analyzing the NMR linewidth behaviours, we confirmed that dimers are more mobile than monomers in these melts. The interplay between the $Al_2Cl_7^-/AlCl_4^-$ ratio and the different moieties mobility makes the 1.2 composition the most interesting to be used as the electrolyte in Al-ion batteries, although a sort of conductivity plateau can be envisaged in the composition range 1.1-1.3. The 1.2 composition was tested in a standard Al-ion cell and gave good results also at high current gravimetric density (222 mA g^{-1}).

ASSOCIATED CONTENT

The following files are available free of charge.

ESI (.pdf file) with ^{13}C and ^{1}H spectra together with attribution.

AUTHOR INFORMATION

* Piercarlo Mustarelli, piercarlo.mustarelli@unipv.it

Author Contributions

C. Ferrara and V. Dall'Asta equally contributed to the work. V. Berbenni performed DSC measurements. C. Ferrara performed NMR measurements. V. Dall'Asta performed conductivity and electrochemical measurements. E. Quartarone and P. Mustarelli planned the research. C. Ferrara and P. Mustarelli wrote the paper. All authors approved the final version of the manuscript.

REFERENCES

1- Dymek, C. J.; Williams, J. L.; Groeger, D. J.; Auborn, J. J. An Aluminum Acid-Base Concentration Cell Using Room Temperature Chloroaluminate Ionic Liquids. *J. Electrochem. Soc.* **1984** *131,* 2887–2892.

2- Auborn, J. J.; Barberio, Y. L. An Ambient Temperature Secondary Aluminum Electrode: Its Cycling Rates and Its Cycling Efficiencies. *J. Electrochem. Soc.* **1985** *132*, 598–601.

3- Giffin, G. A. Ionic Liquid-Based Electrolytes For "Beyond Lithium" Battery Technologies. *J. Mater. Chem. A* **2016** *4*, 13378-13389.

4- Elia, G.A.; Marquardt, K.; Hoeppner, K.; Fantini, S.; Lin, R.; Knipping, E.; Peters, W.; Drillet, J.-F.; Passerini, S.; Hahn, R. An Overview and Future Perspectives of Aluminum Batteries. *Adv. Mater.* **2016** *28*, 7564-7579.

5- Licht, S.; Levitin, G.; Yarnitzky, C.; Tel-Vered, R. The Organic Phase for Aluminum Batteries. *Electrochem. Solid-State Lett.* **1999** *2*, 262–264.

6- Bai, L.; Conway, B. E. Complex Behavior of Al Dissolution in Non-Aqueous Medium as Revealed by Impedance Spectroscopy. *J. Electrochem. Soc.* **1990** *137,* 3737–3747.

7- Boston, C. R.; Hastie, J. W.; Hester, R. E. *Advances in Molten Salt Chemistry*., Springsten US, Boston, MA, USA 1971.

8- Galiński, M.; Lewandowski, A.; Stepniak, I. Ionic liquids as electrolytes. *Electrochimica Acta*, **2006** *51* (26), 5567-5580.

9- Zhang, M.; Kamavaram, V.; Reddy, R. G. New Electrolytes for Aluminum Production: Ionic Liquids. *JOM* **2003** *9*, 54-57.

10- Nakayama, Y.; Senda, Y.; Kawasaki, H.; Koshitani, N.; Hosoi, S.; Kudo, Y.; Morika, H.; Nagamine, M. Sulfone-Based Electrolytes For Aluminum Rechargeable Batteries. *PCCP* **2015** *17*, 5758-5766.

11- Wang, H.; Gu, S.; Bai, Y.; Chen, S.; Zhu, N.; Wu C.; Wu, F. Anion-Effects on Electrochemical Properties of Ionic Liquid Electrolytes For Rechargeable Aluminum Batteries. *J. Mater. Chem. A* **2015** *3*, 22677–22686.

12- Rocher, N. M.; Izgorodina, E. I.; Ruther, T.; Forsyth, M.; MacFarlane, D. R.; Rodopoulos, T.; Horne, M. D.; Bond, A. M. Aluminum Speciation in 1-Butyl-1-Methylpyrrolidinium Bis(Trifluoromethylsulfonyl)amide/$AlCl_3$ Mixtures. *Chem.–Eur. J.* **2009** *15*, 3435–3447.

13- Zein El Abedin, S.; Moustafa, E. M.; Hempelmann, R.; Natter, H.; Endres, F. Additive Free Electrodeposition of Nanocrystalline Aluminum In A Water And Air Stable Ionic Liquid. *Electrochem. Comm.* **2005** *7*, 1111–1116.

14- Eiden, P.; Liu, Q.; Zein El Abedin, S.; Endres, F.; Krossing, I. An Experimental and Theoretical Study of the Aluminum Species Present in Mixtures of $AlCl_3$ with the Ionic Liquid [BMP]Tf_2N and [EMIm]Tf_2N. *Chem.–Eur. J.* **2009** *15*, 3426–3434.

15- Fang, Y.; Yoshii, K.; Jiang, X.; Sun, X. G.; Tsuda, T.; Mehio, N.; Dai, S. An AlCl3 Based Ionic Liquid With a Neutral Substitued Pyridine Ligand For Electrochemical Deposition of Aluminum. *Electrochem. Acta* **2015** *160*, 82–88.

16- Jiang, T.; Chollier Brym, M. J.; Dubé, G.; Lasia, A.; Brisard, G. M. Electrodeposition of Aluminum From Ionic Liquids: Part I – Electrodeposition and Surface Morphology Of Aluminum From Aluminum Chloride ($AlCl_3$)-1-Ethyl-3-Methylimidazolium Chloride ([EMIm]Cl) Ionic Liquids. *Surf. & Coatings Tech.* **2006** *20*1, 1-9.

17- Wilkes, J. S.; Levisky, J. A.; Wilson, R. A.; Hussey, C. L. Dialkylimidazolium Chloroaluminate Melts: A New Class of Room-Temperature Ionic Liquids For Electrochemistry, Spectroscopy and Synthesis. *Inorg. Chem.* **1982** *21*, 1263–1264.

18- Lin, M.-C.; Gong, M.; Lu, B.; Wu, Y.; Wang, D.-Y.; Guab, M.; Angell, M.; Chen., C.; Yang, J.; Hwang, B.-J.; Dai, H. An Ultrafast Rechargeable Aluminum-Ion Battery. *Nature* **2015** *520*, 325-328.

19- Massiot, D.; Fayon, F.; Capron, M.; King, I.; Le Calvé, S.; Alonso, B.; Durand, J. O.; Bujoli, B.; Gan, Z.; Hoatson, G. Modeling One- and Two- Dimensional Solid State NMR Spectra. *Magn. Reson. Chem*. **2002** *40*, 70−76.

20- Ferrari, S.; Quartarone, E.; Tomasi, C.; Bini, M.; Galinetto, P.; Fagnoni, M.; Mustarelli, P. Investigation of ether-based ionic liquid electrolytes for lithium-O2 batteries. *J. Electrochem. Soc.* **2015** *162 (2)*, A3001-A3006.

21- Ferrari, S.; Quartarone, E.; Tomasi, C.; Ravelli, D.; Protti, S.; Fagnoni, M.; Mustarelli, P. Alkoxy substituted imidazolium-based ionic liquids as electrolytes for lithium batteries. *J. Power Sour.* **2013** *235*, 142-147.

22- Ferrari, S.; Quartarone, E.; Mustarelli, P.; Magistris, A.; Fagnoni, M.; Protti, S.; Gerbaldi, C.; Spinella, A. Lithium ion conducting PVdF-HFP composite gel electrolytes based on N-methoxyethyl-N-methylpyrrolidinium bis(trifluoromethanesulfonyl)-imide ionic liquid. *J. Power Sour.* **2010** *195 (2)*, 559-566.

23- Ferrari, S.; Quartarone, E.; Mustarelli, P.; Magistris, A.; Protti, S.; Lazzaroni, S.; Fagnoni, M.; Albini, A. A binary ionic liquid system composed of N-methoxyethyl-N-methylpyrrolidinium bis(trifluoromethanesulfonyl)-imide and lithium bis(trifluoromethanesulfonyl)imide: A new promising electrolyte for lithium batteries. *J. Power Sour*. **2009** *194 (1),* 45-50.

24- Angell, C.A. Entropy and fragility in supercooling liquids. *J. Res. National Inst. Standards and Technology* **1997** *102 (2),* 171-181.

25- *Vila, J.; Ginés, P.; Pico, J.M.; Franjo, C.; Jiménez, E.; Verela, L. M.; Cabeza, O.* Temperature Dependence of the Electrical Conductivity in EMIM-based Ionic Liquids Evidence of Vogel-Tamman-Fulcher Behaviour. *Fluid Ph. Equil.* ***2006*** *242* 141-146.

26- Revel, R.; Audichon, T.; Gonzalez, S. Non-aqueous aluminium-air battery based on ionic liquid electrolyte. *J. Power Sour.* **2014** *272* 415-421.

27- Gray, J. L.; Maciel, G. E. Aluminum-27 Nuclear Magnetic Resonance Study of The Room-Temperature Melt Aluminum Trichloride Butylpyridinium Chloride. *J. Am. Chem. Soc.* **1981** *103*, 7147-7151.

28- Takahashi, S.; Saboungi, M.-L.; Klinger, R.J.; Chen, M.J.; Rathke, J.W. Dynamics of Room-Temperature Melts: Nuclear Magnetic Resonance Measurements of Dialkylimidazolium Haoaluminates. *J. Chem. Soc. Far. Trans.* **1993** *89*, 3591-3595.

29- Wilkes, J.S.; Frye, J. S.; Reynolds, G. F. Aluminum-27 and Carbon-13 NMR Studies Of Aluminum Chloride-Dialkylimidazolium Chloride Molten Salts. *Inorg. Chem.* **1983** *22*, 3870-3872.

30- Černý, Z.; Machàček, J.; Fusek, J.; Čàsenský, B.; Kříž, O.; Tuck, D. G. ^{27}Al NMR Studies of the Hydrolysis of Aluminum(III) Chloride In Non-Aqueous Media. *Inorg. Chim. Acta* **2000** *300-302*, 556-564.

31- Černý, Z.; Machàček, J.; Fusek, J.; Čàsenský, B.; Kříž, O.; Tuck, D. G.; Aluminum-27 and ^{71}Ga NMR studies of the Solution Chemistry of Ga[$AlCl_4$] and Related Compounds. *J. Chem. Soc., Dalton Trans.* **1998** *9*,1439-1446.

32- Zissi, G. D.; Bessada, C. ^{27}Al NMR Spectra of The $RECl_3$-$AlCl_3$ (RE = Y,La) Glasses And Melts. *Z. Naturforsch. A* **2001** *56a*, 697-701.

33- Hinton, J. F.; Briggs, R.W. *NMR and the periodic table*, Academic Press, London 1978, p 281

34- Hu, P.; Zhang, R.; Meng, X.; Liu, H.; Xu, C.; Liu, Z. Structural and Spectroscopic Characterizations of Amide-$AlCl_3$-Based Ionic Liquid Analogues. *Inorg. Chem.* **2016** *55*, 2374-2380.

35- F. Birkenender, R. W. Berg, and N. J. Bjerrum, Acta Chem. Scand. **47,** 344 (1993).

36- Alvarenga, A. D.; Saboungi, M. L.; Curtiss, L. A.; Grimsditch, M.; Structure and Dynamics of Molten Aluminum And Gallium Trihalides. *Molecular Physics* **1994** *81***,** 409-420.

37- Krebs, B.; Greiwing, H.; Brendel, C.; Taulelle, F.; Gaune-Escard, M.; Berg, R. W. Crystallographic and Aluminum-27 NMR Study on Premelting Phenomena in Crystals of Sodium Tetrachloroaluminate. *Inorg. Chem.* **1991** *30***,** 981-988.

38- Sun, X.-G.; Fang, Y.; Jiang, X.; Yoshii, K.; Tsuda, T.; Dai, S. Polymer Gel Electrolytes for Application in Aluminum Deposition and Recheargeable Ion Batteries. *Chem. Comm.* **2016** *52,*292-295.

39- Geetha, S.; Trivedi, D.C.; Properties and applications of chloroaluminate as room temperature ionic liquid. *Bull. Electrochem.* **2003** *19,* 37-48.

40- Hussey, C. L.; Scheffler, T.B.; Wilkers, J. S.; Fannin, A. A. Chloroaluminate Equilibria in the Aluminum Chloride-1-Methyl-3-Ethylimidazolium Chloride Ionic Liquid. *J. Electrochem. Soc.* **1986** *133*, 1389-1391.

41- Karpinski, Z. J.; Osteryoung. R.A., Determination of Equilibrium Constant for the Tetrachloroaluminate Ion Dissociation in Ambient-Temperature Ionic Liquids. *Inorg. Chem.* **1984** *23*, 1491-1494.

42- Jayaprakash, N.; Das, S. K.; Archer, L. A. The Rechargeable Aluminum-Ion Battery. *Chem. Comm.* **2011** *47*, 12610-12612.

TOC